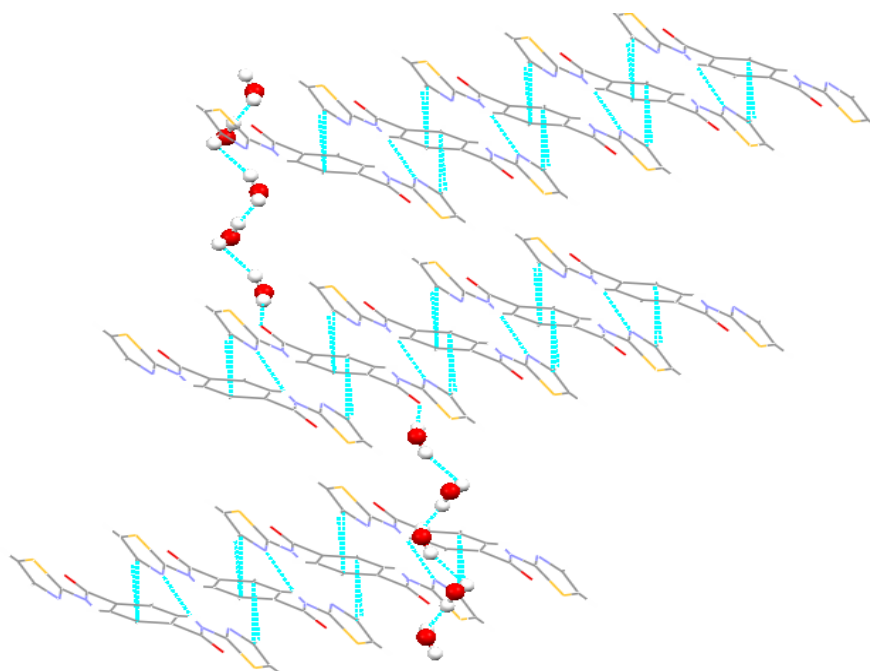


Chapter-6

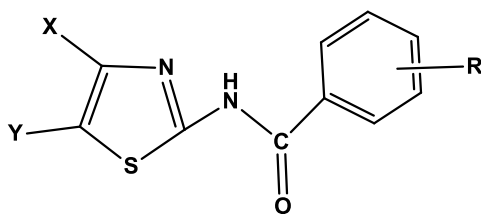


Structure property correlation of supramolecular assemblies organized by Thiazole based amides

6.1 Introduction

Self-assembly driven by Molecular recognition has been studied extensively for more than two decades.¹⁻² Weak Non covalent interactions like hydrogen bonding, electrostatic interaction, π - π stacking, Van der Waals interactions etc. play a critical role in successfully controlling the structures and shapes of the aggregations such as columnar, ribbon, tape, cylindrical and helical architectures.³⁻⁵ Helicity exists in numerous biological and chemical systems; it is among the most elegant architectures found in nature. The α -helical structure is a very common motif in protein. DNA-double helices⁶ and triple helical structures in collagen proteins are also examples of helicity. The Helical structure is stabilized mainly by intramolecular hydrogen bonding. With the purpose of exploring new biological and material functions and applications, chemists have been actively engaged in mimicking this natural structural motif to facilitate the construction of artificial helices.⁷⁻⁹ Construction of supramolecular helical assemblies using various types of noncovalent bonding interactions are of great interest not only from fundamental perspective, but also because it offers potential applications in materials science.¹⁰ In recent years, some supramolecular aggregates that could form helical structure have led to the formation of gels.¹¹ The self-assembled small organic molecules get entangled to form a three-dimensional network that immobilizes the solvent molecules and thereby results in gels or viscous liquids.¹²⁻¹³ Supramolecular gel has been demonstrated as one of the competent ways of obtaining chiral nanostructures in a large quantity.¹⁴⁻¹⁵

A series of thiazole based amide derivatives synthesized by various aliphatic acids (decane carboxylic acid to octadecane carboxylic acid) and thiazole derivatives has been discussed in previous chapter. We proposed the crucial role of the methyl functionality in inducing the gelation as well as proved to be a deterrent to gelation of various solvent depend on its position on thiazole moiety. In addition, critical aliphatic chain was also essential to induce gelation/nongelation. Consequently, we decided to explore thiazole based amides having aromatic backbone (**Figure 6.1**), since it might provide an opportunity to study the role of π - π interaction in inducing supramolecular gelation along with other weak non-covalent interactions such as (methyl) C-H... π , (methyl)C-H...N, (methyl)C-H...S. Moreover, supramolecular synthon approach is established as a useful tool in designing new gelator molecules.¹⁶



1a, X=H, Y=H, R=H

1b, X=H, Y=H, R=2-CH₃

1c, X=H, Y=H, R=3-CH₃

1d, X=H, Y=H, R=4-CH₃

2a, X=CH₃, Y=H, R=H

2b, X=CH₃, Y=H, R=2-CH₃

2c, X=CH₃, Y=H, R=3-CH₃

2d, X=CH₃, Y=H, R=4-CH₃

3a, X=H, Y=CH₃, R=H

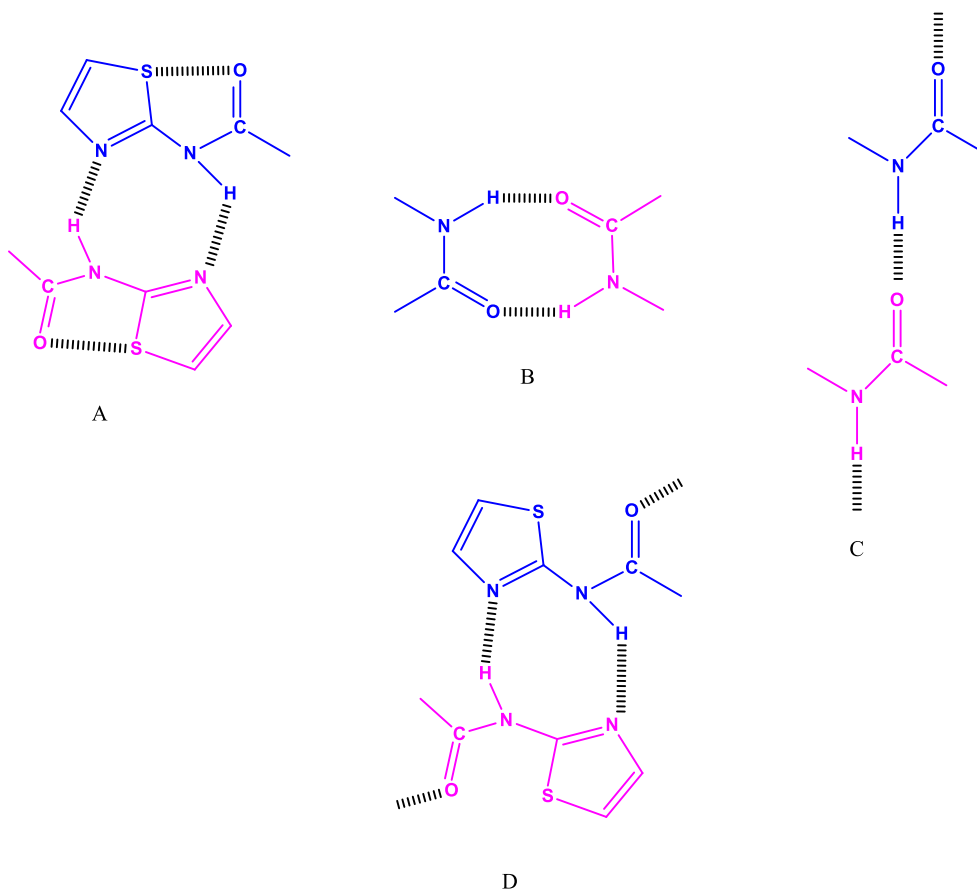
3b, X=H, Y=CH₃, R=2-CH₃

3c, X=H, Y=CH₃, R=3-CH₃

3d, X=H, Y=CH₃, R=4-CH₃

Figure 6.1 N-(thiazol-2-yl)benzamide derivatives

Supramolecular synthon containing intermolecular cyclic N-H...N interaction and intramolecular O...S interaction (**Scheme-6.1, A**) encountered quite often in thiazole based amides as observed in previous chapter.



Scheme 6.1 Probable Supramolecular synthons in amide moiety

It would be interesting to study if this synthon is robust enough to be present in thiazole based amide having aromatic backbone or how predictable is other supramolecular synthons of amide (**Scheme 6.1, B, C, and D**) in the presence of competitive cyclic N-H...N interaction in thiazole based amides.

Thiazole based amides have emerged as a reasonably robust scaffold as gelator. Moreover, Self-assembled diamide derivatives are reported in literature as a potential candidate for inducing gelation.¹⁷⁻¹⁸ These informations prompted us to study the effect of diamide functionality on gelation behaviour of N,N'-di(thiazol-2-yl)phthalamide derivatives (**Figure 6.2**). As discussed formerly Supramolecular synthon containing intermolecular cyclic N-H...N interaction observed frequently in thiazole based amides. Hence it is expected to perceive the N-H...N interaction in thiazole based diamide also. As it is evident from the **scheme 6.2** that thiazole based diamide moiety can form synthon A if cyclic N-H...N interaction is absent. Whereas, the presence of cyclic N-H...N interaction leads to synthon B.

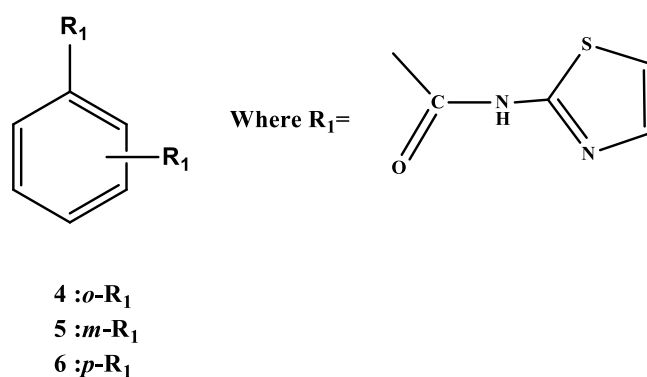
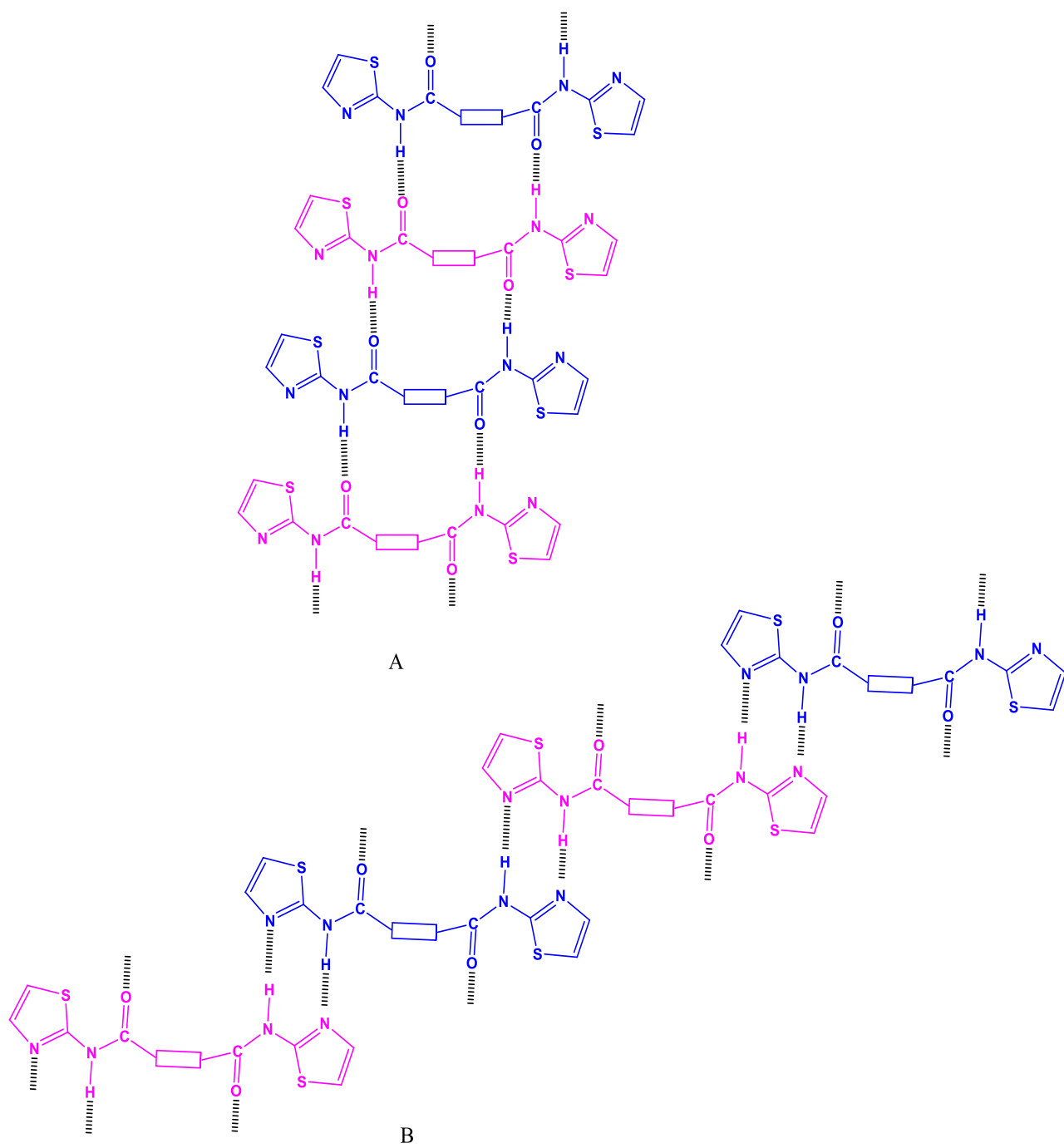


Figure 6.2 N,N'-di(thiazol-2-yl)phthalamide derivative



Scheme 6.2 Probable Supramolecular synthons in diamide moiety

6.2 Experimental Section

6.2.1 Materials and physical measurements

6.2.1.1 Materials

2-Aminothiazole (97%), 2-Amino-5-methylthiazole (98%), 2-Amino-4-methylthiazole (98%), benzoic acid (97%), 2-toluic acid (98%), 3-toluic acid (98%), 4-toluic acid (99%), phthaloyl dichloride (97%), isophthaloyl dichloride (98%), terephthaloyl dichloride (98%) (All from Aldrich) were used as received. The other chemicals were of the highest commercial grade available and were used without further purification. The solvents used for the preparation of gels were reagent grade. All solvents used in the synthesis were purified, dried and distilled as required.

6.2.1.2 FTIR spectroscopy

FTIR Spectra were recorded on a Perkin Elmer –RX FTIR instrument. Solid samples were recorded as an intimate mixture with powdered KBr.

6.2.1.3 NMR spectroscopy

The ^1H - NMR spectra were measured by using a Bruker AVANCE, 400MHZ for ^1H -NMR with TMS as internal standard.

6.2.1.4 Scanning Electron Microscopic Study

Morphologies of all reported gel materials were investigated using scanning electron microscopy (SEM). For SEM study, the gel materials were dried to give xerogel, followed by recording the micrographs in a SEM apparatus (JEOL JSM5610 LV microscope)

6.2.1.5 Single Crystal X-ray studies

Single crystal X-ray study was carried out on Single Crystal X-ray diffractometer (Xcalibur, EOS, Gemini diffractometer). All structures were solved and refined using the Olex2¹⁹ software and ShelXL²⁰ refinement package Graphics are generated using MERCURY 3.0. All structures are solved by direct methods and refined in a routine manner. In all cases, nonhydrogen atoms are treated anisotropically. Whenever possible, the hydrogen atoms are located on a difference Fourier map and refined. In other cases, the hydrogen atoms are geometrically fixed.

6.2.1.6 Gelation Test

A weighted amount of potential gelator and a measured volume of selected pure organic solvent were placed into a test tube, and the system was heated in oil or water bath until all solid materials were dissolved. The solution was cooled to room temperature and finally, the test tube was turned upside down to observe if the solution inside could still flow. A positive test is obtained if the flow test is negative. Systems in which only solution remained until the end of the tests are referred as solutions (S). Systems that are clear solutions when they are hot but precipitation or crystallization occurs when they are cooled down to room temperature are denoted by P (precipitation) and R (recrystallization), respectively.

6.2.1.7 T_{gel} Measurement

Temperatures of gel-to-sol transition (T_{gel}) were determined by using a conventional “falling ball” method. In this test, a small glass ball (63mg) was carefully placed on the top of the gel to be tested, which was produced in a test tube. The tube was slowly heated in a thermostated oil bath until the ball fell to the bottom of the test tube. The temperature at which the ball reaches to the bottom of the test tube is taken as T_{gel} of that system.

6.2.2 Synthetic procedure

6.2.2.1 Synthesis method of N-(thiazol-2-yl)benzamide derivatives

Oxalyl chloride (2ml, 20 mmol) was added slowly to a stirred solution of Monocarboxylic Acids (2 mmol) in dry dichloromethane (10mL) under a nitrogen atmosphere, and stirring was continued under a nitrogen atmosphere for 12 h. Excess oxalyl chloride and solvent were removed by distillation under reduced pressure. The acid chloride obtained was dissolved in dry dichloro methane (10 mL) and added to the aminothiazole (2 mmol) in triethylamine (0.3ml, 2.15mmol). The mixture was stirred under a nitrogen atmosphere for overnight. The reaction mixture was then added to dilute hydrochloric acid (5%), and extracted with chloroform. The product residue after removing chloroform was purified by repeated crystallization from ethanol.

6.2.2.2 Synthesis method of N,N'-di(thiazol-2-yl)phthalamide derivatives

The synthesis was carried out using a modified synthetic procedure.²¹ Two equivalent solution of (0.80 g, 8.0 mmol) 2-aminothiazole in 20 mL of freshly distilled THF at

0°C was added slowly to a solution of (0.81 g, 4.0 mmol) acid chloride in 50 mL of freshly distilled THF and a precipitation was formed immediately. After 10 minutes (20 mmol) triethylamine was added, and the solution was stirred for another 30 minutes at room temperature. The solution was then heated at reflux for 2-3 hr and after cooling to room temperature the precipitate obtained was washed with aqueous HCl solution. The product was purified by multiple washing with chloroform.

6.2.3 Analytical data

1a: Yield 69%, m.p. 183°C, ¹HNMR (400 MHz, CDCl₃, TMS): δ8.262 (d, 2H; CH), 8.188(d, 1H; CH), 7.652(d, 1H; CH), 7.614(d, 1H, CH), 7.533 (t, 2H, CH), 7.068(d, 1H; CH).FTIR (KBr): 3448,3136,2676,1698,1678,1572,1526,1500,1453, 1425,1350, 1326, 1294 , 1256, 1180,1144,1071,1027,934,832,760,707,667,559,490,421cm⁻¹.

1b: Yield 73%, m.p. 172°C, ¹HNMR (400 MHz, CDCl₃, TMS): δ13.210(s, 1H; NH), 7.572 (d, 1H; CH), 7.496(t, 1H; CH), 7.357(m, 2H; CH), 6.813(d, 1H, CH), 6.280(t, 1H, CH), 2.506(s, 3H; CH₃).FTIR (KBr):3452,3147,3105,2945, 1762,1688, 1565,1486, 1412 ,1367, 1305,1283, 1168,1044,891,836, 801,734,706,665,560, 524, 452 cm⁻¹.

1c: Yield 67%, m.p. 132°C, ¹HNMR (400 MHz, CDCl₃, TMS): δ7.976 (d, 1H; CH), 7.479(d, 2H; CH), 7.401 (d, 1H; CH), 7.083(d, 1H; CH), 2.459(s, 3H; CH₃).FTIR (KBr): 3411, 3166,2916,1756,1671,1548,1487,1324,1291,1192, 1165, 1108, 1062, 999, 930, 875,823,801,765,723,700,676,521,461cm⁻¹.

1d: Yield 79%, m.p. 189°C, ¹HNMR (400 MHz, CDCl₃, TMS): δ8.046 (d, 2H; CH), 7.437(d, 2H; CH), 7.074(d, 1H; CH), 2.474(d, 3H, CH₃).FTIR (KBr): 3409, 3153,2945, 1764, 1666,1611,1541,1487,1439,1397,1372,1301, 1166,1109,1057, 894, 831,737, 685,626, 583,523,484,431cm⁻¹.

2a: Yield 68%, m.p. 106°C, ¹HNMR (400 MHz, CDCl₃, TMS): δ8.132 (d, 2H; CH), 7.699(t, 2H; CH), 7.609(t, 1H; CH), 6.695(s, 1H, CH), 2.546 (s, 3H, CH₃). FTIR (KBr): 3435, 2923,2360,1611,1519,1481,1435,1416,1370,1304,1172, 1112,991, 964, 833,758, 727, 696,622,552,511,433 cm⁻¹.

2b: Yield 69%, m.p. 100°C, ¹HNMR (400 MHz, DMSO, TMS): δ 7.736 (d, 1H; CH), 7.489(d, 1H; CH), 7.356(m, 2H; CH), 6.611(s, 1H, CH), 2.261(s,3H, CH₃), 2.310 (s,3H,CH₃)

FTIR(KBr):3238,3149,3045,2919,2797,1924,1770,1673,1562,1562,1556,1490,1452,1379,13151254,1167,1137,1044,993,946,891,807,746,673,657,620,529,452 cm⁻¹.

2c: Yield 71%, m.p. 96°C, ¹HNMR (400 MHz, CDCl₃, TMS): δ8.262 (d, 2H; CH), 8.188(d, 1H; CH), 7.652(d, 1H; CH), 7.614(d, 1H, CH), 7.533 (t, 2H, CH), 7.068(d, 1H;CH).

FTIR(KBr):3180,3058,2918,2357,1688,1585,1550,1466,1410,1379,1311,1279,1211,1166,1111, 1087,956,832,786,722,672,626,527,417cm⁻¹.

2d: Yield 73%, m.p. 118°C, ¹HNMR (400 MHz, CDCl₃, TMS): δ7.984 (d, 2H; CH), 7.333(d, 2H; CH), 6.964 (s, 1H, CH), 2.443(s, 6H; CH₃). FTIR (KBr): 3449, 3169, 2846, 1743,1682, 1560,1492,1462,1422,1375, 1340,1319, 1275,1172,1114,1063, 960, 874, 803, 778, 714,627,520cm⁻¹.

3a: Yield 78%, m.p. 135°C, ¹HNMR (400 MHz, CDCl₃, TMS): δ8.329 (d, 2H; CH), 7.722(t, 1H; CH), 7.628(t, 2H; CH), 7.258(s, 1H, CH), 2.529 (s, 3H, CH₃).

FTIR(KBr):3411,3160, 3057, 2918,2849,1770,1671,1550,1449,1396,1309,1160,1076, 044,931,891,839, 796,755,698,529,409 cm⁻¹.

3b: Yield 69%, m.p. 188°C, ¹HNMR (400 MHz, DMSO, TMS): δ12.328 (s, 1H; NH), 7.520 (d, 1H; CH), 7.438(t, 1H; CH), 7.323(m, 2H; CH), 7.186(s, 1H, CH), 2.376 (s, 6H,CH₃).

FTIR (KBr):3266,3170,3080,2917,2849,2734,2360,1676,1575,1492,1468,1420,1378 , 1338,1321,1262,1248,1194,1166,1141,1109,1065,659,874,805,778,718,694,634,605, 520,477cm⁻¹.

3c: Yield 78%, m.p. 106°C, ¹HNMR (400 MHz, CDCl₃, TMS): δ8.061 (d, 1H; CH), 7.971(d, 1H; CH), 7.466(d, 2H; CH), 7.145(s, 1H, CH), 2.487-2.322 (d, 6H, CH₃).FTIR(KBr):182,3061,2952,2899,2815,1724,1667,1559,1480,1311,1208,1153,1079,986,930,892, 866,826,743,674,547,493,434cm⁻¹.

3d: Yield 76%, m.p. 110°C, ¹HNMR (400 MHz, CDCl₃, TMS): δ7.984 (d, 2H; CH), 7.333(d, 2H; CH), 6.964 (s, 1H, CH), 2.443(s, 6H; CH₃).FTIR (KBr): 3214,

2919,2863,2345,1814, 1690,1669,1611,1566,1515, 1419,1313,1215,1178,1158, 1125, 1020,961,893,834,756, 680.608,543,526,469 cm^{-1} .

4: Yield 81%, m.p. 196°C, ^1H NMR (400 MHz, DMSO, TMS): δ 12.735 (s, 2H; NH), 7.787(d, 2H; CH), 7.658(d, 2H; CH), 7.536(d, 2H, CH), 7.269 (d, 2H, CH).FTIR (KBr):3448,3136,2676,1698,1678,1572,1526,1500,1453,425,1350,1326,1294,1256, 1180, 1144, 1071,1027,934,832,760,707,667,559,490,421 cm^{-1} .

5: Yield 79%, m.p. 204°C, ^1H NMR (400 MHz, DMSO, TMS): δ 13.008(s, 2H; NH), 8.649 (s, 1H; CH), 8.308(d, 2H; CH), 8.176(d, 1H, CH), 7.591(m, 2H, CH), 7.300(d, 2H; CH). FTIR (KBr):3452,3147,3105,2945, 1762,1688, 1565,1486, 1412 ,1367, 1305,1283, 1168,1044,891,836,801,734,706,665,560,524,452 cm^{-1} .

6: Yield 84%, m.p. 243°C, ^1H NMR (400 MHz, DMSO, TMS): δ 12.901 (s, 2H; NH), 8.216(s, 4H; CH), 7.587 (d, 2H; CH), 7.319(d, 2H; CH). FTIR (KBr): 3411, 3166, 2916, 1756, 1671, 1548, 1487, 1324, 1291, 1192, 1165, 1108, 1062,999, 930,875,823, 801, 765, 723,700,676,521,461 cm^{-1} .

6.3 Results and discussion

6.3.1 Gel Formation and Characterization

All the synthesized compounds were subjected to gelation test in various solvents with varied polarity ranging from highly polar solvents such as water, ethanol, methanol to very less polar solvents such as toluene and n-octadecane (**Table 6.1**). It is clear from Table 6.1 that among the series of synthesized compounds only two (1c and 3c) turned out to be fairly good gelator for ethanol/water (1:1) or methanol/water (1:1) mixture. 1c and 3c showed quite low minimum gel concentration (MGC) for the gelation of methanol/water or ethanol/water mixture (**Table 6.1**).

Table 6.1

Solvent	1a	1b	1c	1d	2a	2b	2c	2d
Ethanol	S	S	S	S	S	S	S	S
Methanol	S	S	S	S	S	S	S	S
Water	P	P	P	P	P	P	P	P
Ethanol/Water (1:1)	C	C	G (1.08)	C	C	C	C	C
Methanol/Water (1:1)	C	C	G (1.02)	C	C	C	C	C
DMF	S	S	S	S	S	S	S	S
Iso-octane	P	P	P	P	P	P	P	P
n-octadecane	S	S	S	S	S	S	P	S
DMSO	S	S	S	S	S	S	S	S
Toluene	P	P	S	S	S	S	S	S
Xylene	P	P	P	P	P	P	P	P

Solvent	3a	3b	3c	3d	4	5	6
Ethanol	S	S	S	S	I	I	I
Methanol	S	S	S	S	I	I	I
Water	P	P	P	P	I	I	I
Ethanol/Water (1:1)	C	C	G (2.03)	C	I	I	I
Methanol/Water (1:1)	C	C	G (1.93)	C	I	I	I
DMF	S	S	S	S	S	S	S
Iso-octane	P	P	P	P	I	I	I
n-octadecane	P	S	S	S	I	I	I
DMSO	S	S	S	S	S	S	S
Toluene	P	P	S	S	I	I	I
Xylene	P	P	P	P	I	I	I

G=gel, P=precipitate, C=crystals, S=solution, I=Insoluble, values in the parenthesis represent MGC (minimum gelator concentration) in wt % (g/100mL of solvent)

A graph of T_{gel} versus concentration of gelator molecules in wt% (w/v) showed a gradual increase in T_{gel} up to a certain concentration of gelator then plateau was observed (**Figure 6.3**). Understandably, the increase in gelator concentration improves the self-aggregation and stability of supramolecular assembly not beyond certain critical concentration. The nature of the graph for T_{gel} versus concentration of gelator is very frequent for supramolecular gelators.

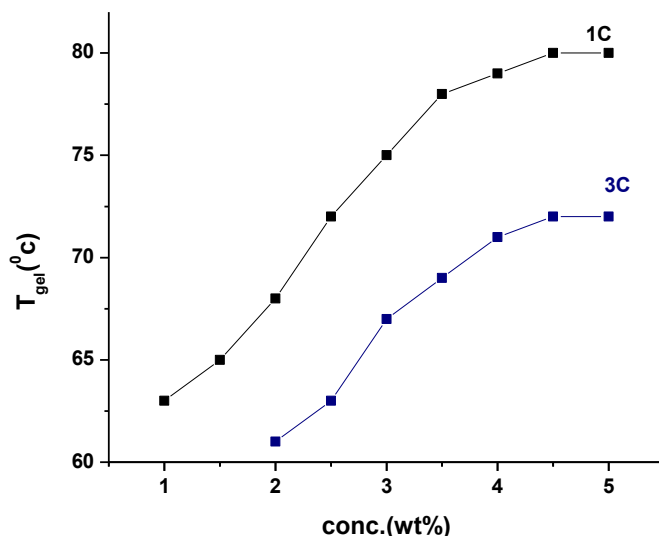


Figure 6.3 Effect of gelators **1a** and **1e** concentration (in wt %) on sol-to-gel transition Temperature (T_{gel})

To study the morphology of gelator fibres a detailed SEM analysis was carried out on xerogel (dried gel) of **1c** and **3c** obtained from ethanol/water (1:1) gel (**Figure 6.4**). SEM image of xerogel of **1c** displayed highly cross linked intertwined twisted fibres. Whereas, the xerogel of **3c** showed a well-defined independent assembly of rod like morphology. Presumably, such loose collections of crystalline tubes immobilize solvents, resulting in a weak gel. Understandably, highly cross linked network of fibres would be capable of hardening a solvent easily than a bundle of rods, which lacks a junction point and or/cross linking.

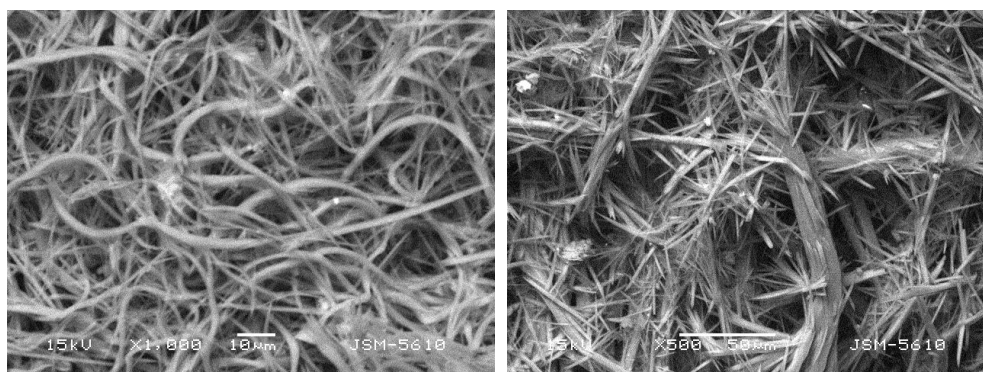


Figure 6.4 SEM images of xerogel of (a) 1c and (b) 3c from 1:1 ethanol/water mixture

6.3.2 Single-Crystal Structures

1. Crystal Structure of 2-methyl-N-(thiazol-2-yl) benzamide (1b). 1b crystallizes in the orthorhombic space group $Pccn$. The two species are strongly hydrogen-bonded with each other through cyclic N-H...N (thiazole) ($N...N = 2.951 \text{ \AA}$, $\angle N-H...N = 175.93^\circ$) and N-H...N (thiazole) ($N...N = 2.951 \text{ \AA}$, $\angle N-H...N = 175.93^\circ$) interactions, along with the intramolecular bond between the carbonyl oxygen atom and the thiazole sulphur atom ($C...S = 2.719 \text{ \AA}$), resulting in a 0D network. Short contacts C-H... π (bond distance = 3.722 \AA , bond angle = 158.01°), C-H... π (bond distance = 3.753 \AA , bond angle = 150.02°), cyclic C-H (thiazol)... π (thiazol) (bond distance = 3.373 \AA), interactions propagates in two directions, resulting in 2D hydrogen bonded chains (**Figure 6.5a**).

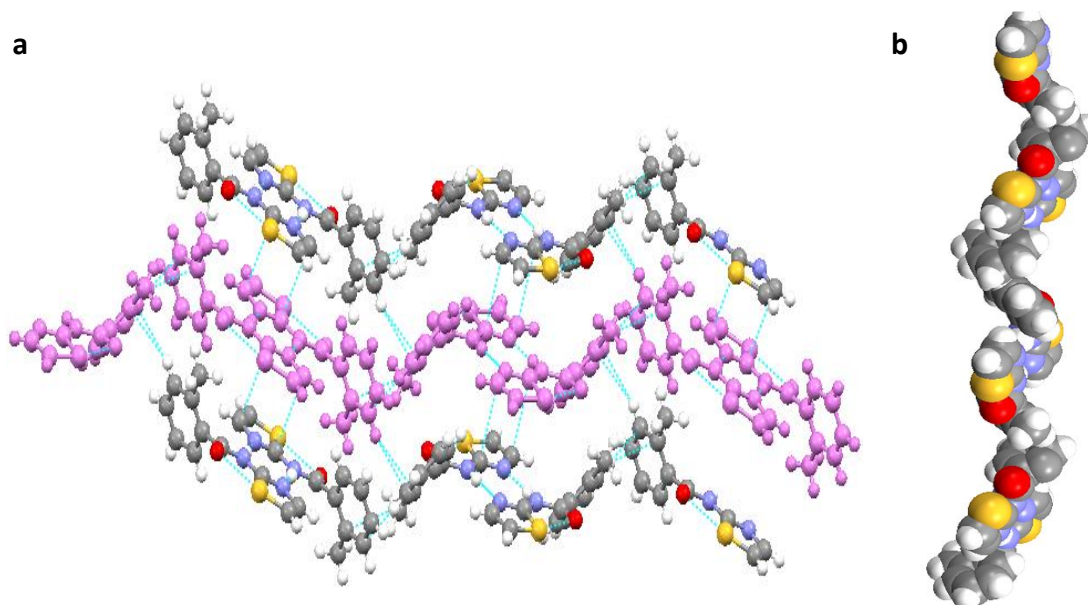


Figure 6.5 view of a) hydrogen bonded helical network of 1b in ball and sticks model and b) Space fill model

A critical examination of the crystal structures verified that, the intermolecular hydrogen bonds propagate in twisted or helical fashion (**Figure 6.5b**).

2. Crystal Structure of 3-methyl-N-(thiazol-2-yl) benzamide (1c). 1c crystallizes in the triclinic space group P -1. The two species are strongly hydrogen-bonded with each other through cyclic N-H.....N (thiazole) ($N\dots N = 2.927 \text{ \AA}$, $\angle N-H\dots N = 150.02^\circ$) and N-H...N (thiazole) ($N\dots N = 3.008 \text{ \AA}$, $\angle N-H\dots N = 151.79^\circ$) interactions, along with the intramolecular bond between the carbonyl oxygen atom and the thiazole sulphur atom ($C\dots S = 2.675 \text{ \AA}$), resulting in a 0D network. Short contacts C.....O ($C\dots O = 3.213 \text{ \AA}$), (methyl)C-H.....O ($C\dots O = 2.683 \text{ \AA}$, $\angle C-H\dots O = 126.71^\circ$), $\pi\dots\pi$ (bond distance = 3.391 \AA), S.....S ($S\dots S = 3.461 \text{ \AA}$), interactions propagates in two directions, resulting in 2D hydrogen bonded chains (**Figure 6.6a**). Interestingly the self-assembly displayed double helix structure (**Figure 6.6b**).

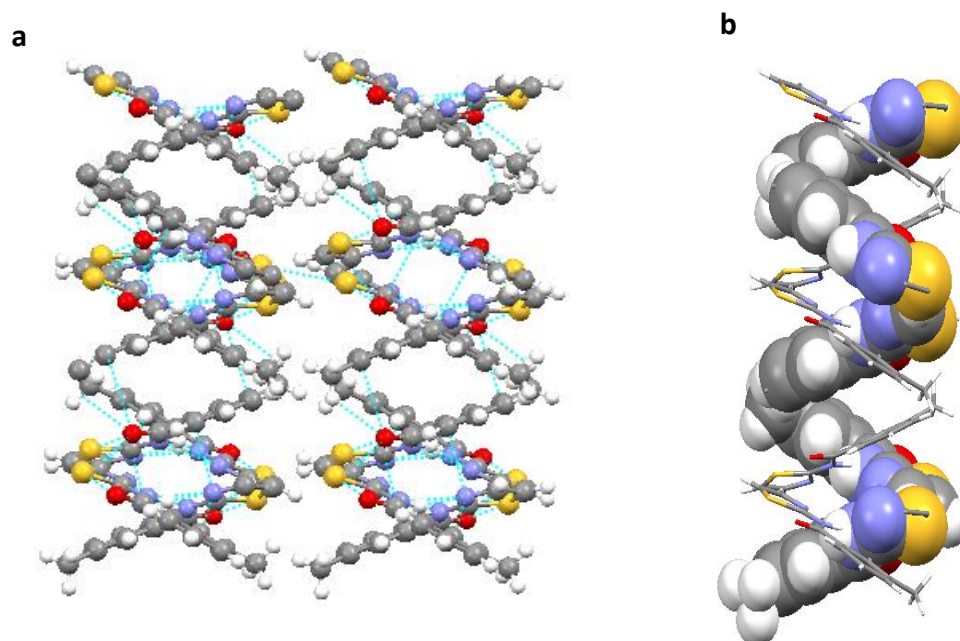


Figure 6.6 view of a) hydrogen bonded double helical network of 1c in ball and sticks model and b) Space fill model

3. Crystal Structure of 4-methyl-N-(thiazol-2-yl) benzamide (1d). 1d crystallizes in the triclinic space group P-1. The two species are strongly hydrogen-bonded with each other through cyclic N-H.....N (thiazole) ($N\dots N = 2.955 \text{ \AA}$, $\angle N-H\dots N = 155.91^\circ$) and N-H...N (thiazole) ($N\dots N = 2.934 \text{ \AA}$, $\angle N-H\dots N = 166.84^\circ$) interactions, along with the intramolecular bond between the carbonyl oxygen atom and the thiazole

sulphur atom ($C\dots S=2.668 \text{ \AA}$), resulting in a 0D network. Short contacts $C-H\dots S$ ($C\dots S =3.884 \text{ \AA}$, $\angle C-H\dots S =171.84^\circ$), $C-H\dots N$ ($C\dots N =3.428 \text{ \AA}$, $\angle C-H\dots N =150.94^\circ$) interactions propagates in one directions, resulting in 1D hydrogen bonded twisted structure (**Figure 6.7a**), While $C-H\dots \pi$ ($C\dots C=3.841 \text{ \AA}$, $\angle C-H\dots C= 133.39^\circ$) interactions propagates, leading to 2D hydrogen bonded network (**Figure 6.7b**).

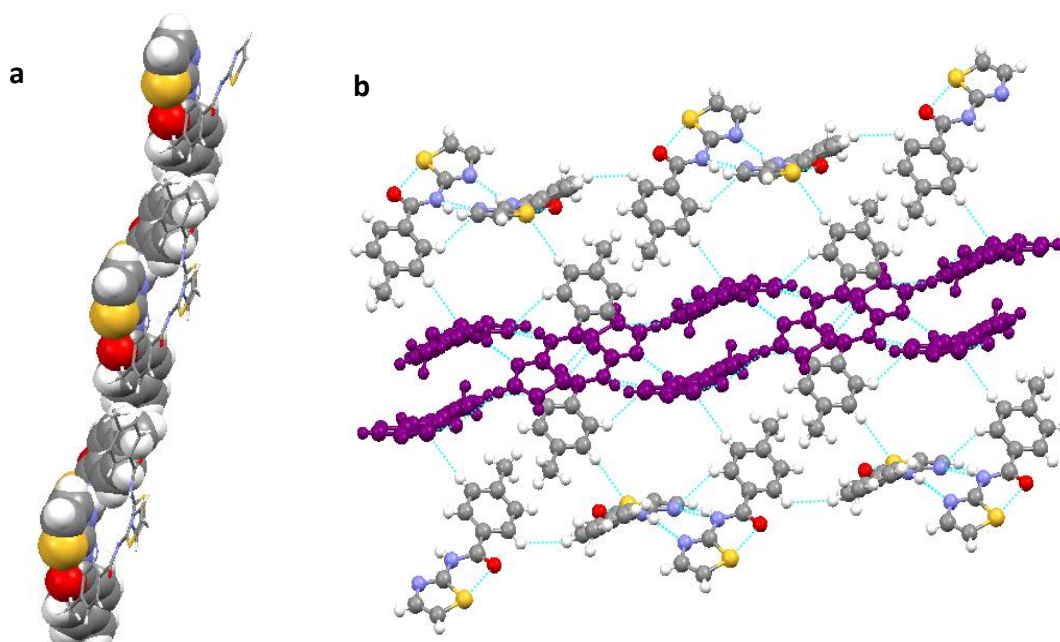


Figure 6.7 view of hydrogen bonded network of 1d, resulting twisted structure a) space fill model and b) ball and sticks model

4. Crystal Structure of 2-methyl-N-(5-methylthiazol-2-yl) benzamide (3b). 3b crystallizes in the triclinic space group P-1. The two species are hydrogen-bonded through cyclic $N-H\dots N$ (thiazole) ($N\dots N =2.871 \text{ \AA}$, $\angle N-H\dots N =155.91^\circ$) interactions, along with the intramolecular bond between the carbonyl oxygen atom and the thiazole sulphur atom ($C\dots S=2.769 \text{ \AA}$), resulting in a 0D network. Short contacts cyclic $C-H\dots O$ ($C\dots O =3.484 \text{ \AA}$, $\angle C-H\dots O=145.06^\circ$) interactions propagates in one directions, resulting in 1D hydrogen bonded helical or twisted chain, While (methyl) $C-H\dots O$ ($C\dots O=3.439 \text{ \AA}$, $\angle C-H\dots O =140.25^\circ$) interactions propagates, the assembly in 2Dimension (**Figure 6.8**).

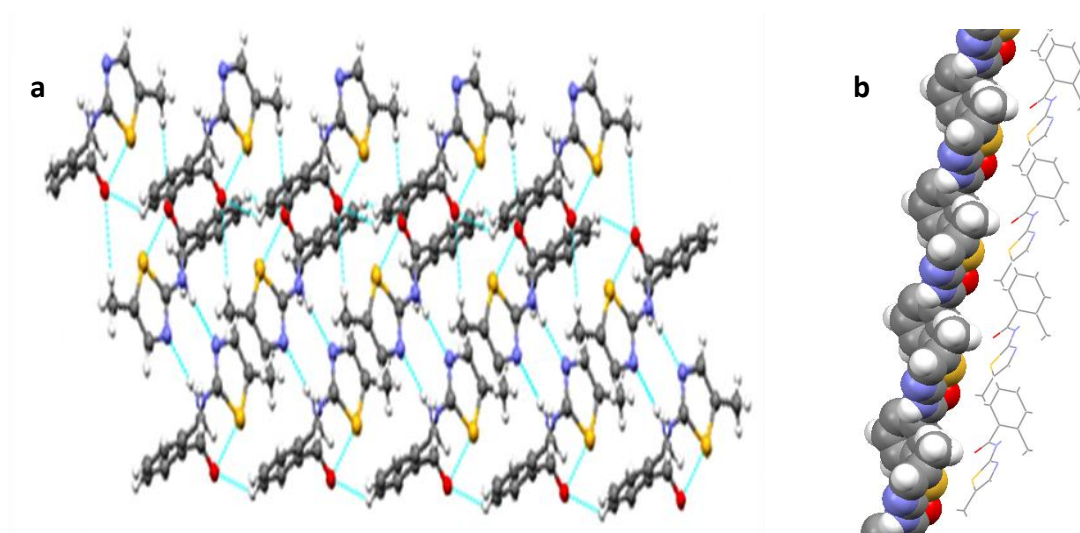


Figure 6.8 view of a) hydrogen bonded network of 3b in ball and sticks model and b) Space fill model

5. Crystal Structure of 4-methyl-N-(5-methylthiazol-2-yl) benzamide (3d). 3d crystallizes in the triclinic space group P-1. The two species are bonded through hydrogen bonding with each other by cyclic N-H.....N (thiazole) ($N\dots N = 3.996 \text{ \AA}$, $\angle N-H\dots N = 148.97^\circ$) and N-H...N (thiazole) ($N\dots N = 2.991 \text{ \AA}$, $\angle N-H\dots N = 149.51^\circ$) interactions, along with the intramolecular bond between the carbonyl oxygen atom and the thiazole sulphur atom ($C\dots S = 2.696 \text{ \AA}$), resulting in a 0D network. Short contacts (methyl)C-H.....C ($C\dots C = 3.685 \text{ \AA}$, $\angle C-H\dots C = 171.06^\circ$), (methyl)C-H..... π (bond distance = 3.578 \AA , bond angle = 145.49°), C-H.....O ($C\dots O = 3.312 \text{ \AA}$, $\angle C-H\dots O = 132.80^\circ$) interactions propagates, leading to 2D hydrogen bonded network (**Figure 6.9**). Though the self-assembly did not propagated in helical manner but it showed consecutive double turn conformation.

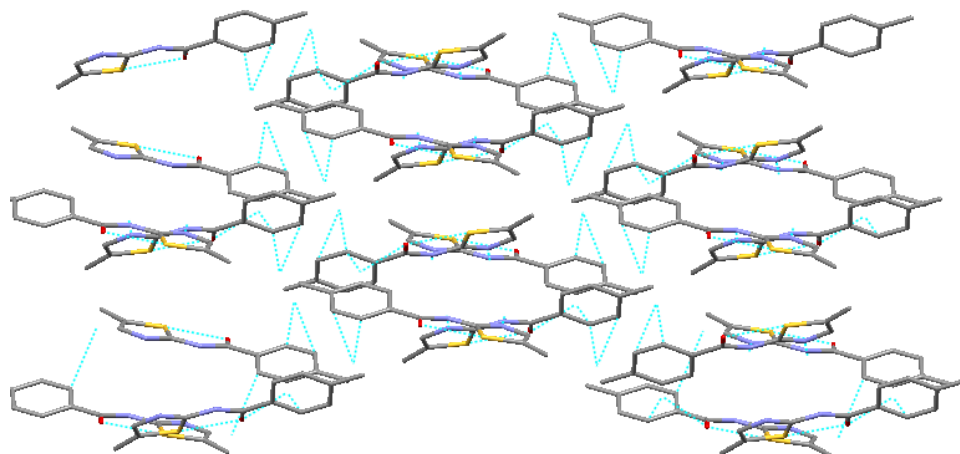


Figure 6.9 view of hydrogen bonded helical network of 3d in capped stick model

6. Crystal Structure of N,N'-di(thiazol-2-yl)terephthalamide (6). 6 crystallize in the monoclinic space group P 21/c. The two species are hydrogen-bonded through cyclic N-H...N (thiazole) ($N...N = 2.941 \text{ \AA}$, $\angle 170.95^\circ$) interactions, along with the intramolecular bond between the carbonyl oxygen atom and the thiazole sulphur atom ($C...S = 2.698 \text{ \AA}$), resulting in a 0D network. While Short contacts $\pi... \pi$ (bond distance $= 3.362 \text{ \AA}$), $C-H... \pi$ ($C...C = 2.778 \text{ \AA}$, $\angle C-H... \pi = 121.83^\circ$), interactions propagates, leading to 1D hydrogen bonded network. Interestingly hydrogen bond between (C=O) O.....O-H (H_2O) ($O...O = 2.850 \text{ \AA}$, $\angle O.....O-H = 176.00^\circ$) proceed as a link to form 2d hydrogen bonded (**Figure 6.10**). Crystallographic parameters are listed in **Table 6.2**.

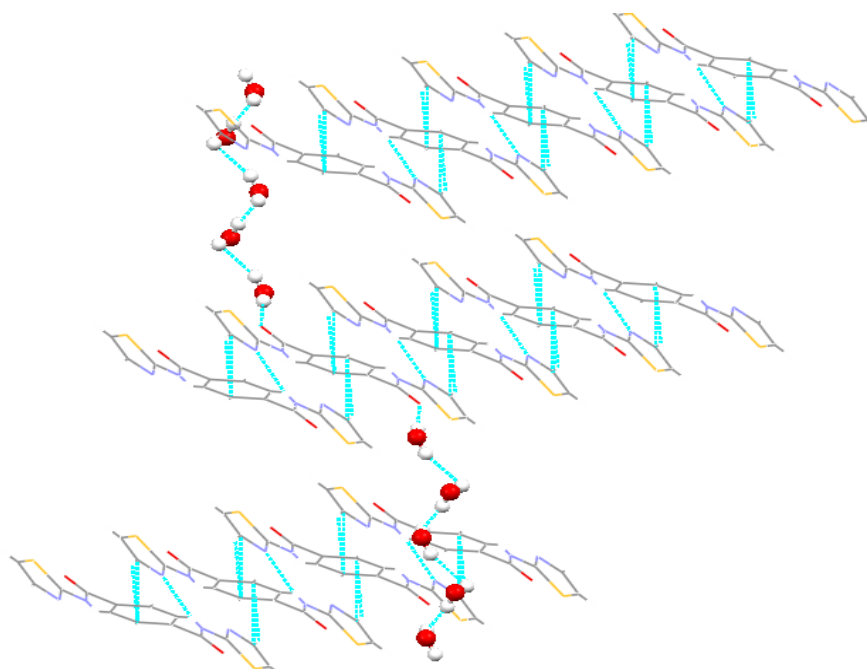


Figure 6.10 view of 2D-hydrogen bonded network of 6 in wireframe model

A critical analysis of weaker interactions (**Table 6.3**) clearly shows the presence of robust cyclic (amide) N-H...N (thiazole) supramolecular synthon leading to 0-D hydrogen bonded network in all the crystal structures. Similarly, the C=O...S (intramolecular) forces found in every crystal structures of thiazole amide, with or without a methyl functional group, appeared to force the long alkyl chain to be almost linear with respect to thiazole moiety.

Table 6.2 crystal parameters

Crystal data	1b	1c	1d	3b	3d	6
Empirical formula	C ₄₄ H ₄₀ N ₈ O ₄ S	C ₂₂ H ₂₀ N ₄ O ₂ S ₂	C ₄₄ H ₄₀ N ₈ O ₄ S ₄	C ₁₂ H ₁₂ N ₂ O S	C ₂₄ H ₂₄ N ₄ O ₂ S ₂	C ₇ H ₇ N ₂ O ₂ S,H ₂ O
Formula weight	873.12	436.56	873.12	232.31	464.62	183.21
Crystal size (mm)	0.67x 0.26 x 0.18	0.48x 0.29 x 0.20	0.85x 0.78 x 0.23	0.23x 0.21 x 0.19	0.24x 0.13 x 0.10	0.6x 0.45 x 0.15
Crystal system	orthorhombic	triclinic	triclinic	triclinic	triclinic	monoclinic
Space group	P c c n	P -1	P -1	P -1	P -1	P 21/c
a/Å	26.1900(7)	7.6161(5)	7.9116(5)	7.4241(3)	7.9795(3)	9.4236(3)
b/Å	13.9209(4)	10.3838(6)	10.6155(5)	8.6102(4)	11.4361(3)	17.2363(6)
c/Å	5.7861(2)	14.0990(7)	13.7731(6)	9.5123(5)	13.6843(5)	4.99730(18)
α/°	90	74.544(5)	72.879(4)	92.070(4)	105.768(2)	90
β/°	90	87.678(5)	75.812(5)	99.897(4)	106.946(3)	100.028(3)
γ/°	90	87.888(5)	82.601(4)	96.537(4)	90.007(2)	90
Volume/ Å ³	2109.53(11)	1073.40(11)	1069.75(10)	594.14(5)	1145.31(6)	799.30(5)
Z	2	2	1	2	2	1
D _{calc}	1.3745	1.3506	1.3552	1.2984	1.3471	1.5224
F(000)	917.1646	458.5823	458.5823	244.3376	488.6753	382.4973
μ (mm ⁻¹)	2.509	2.466	2.474	0.252	0.262	3.282
Temperature (K)	298	293	293	293	293	293
Observed reflection [I > 2σ(I)]	3740	2700	4096	4843	9571	1850
Parameters refined	136	280	299	146	292	120
Goodness of fit	1.1057	0.9007	1.0936	0.7588	0.9111	0.7428
Final R ₁ on observed data	0.0436	0.0557	0.0484	0.0431	0.0508	0.0420
Final wR ₂ on observed data	0.1404	0.2026	0.1510	0.1787	0.2211	0.1637
Source	Cu K _α	Cu K _α	Cu K _α	Mo K _α	Mo K _α	Cu K _α
Wavelength (Å)	1.5418	1.5418	1.5418	0.7107	0.7107	1.5418
CCDC No.	958804	972288	964475	994091	994092	964474

A crucial examination of the crystal structures demonstrated presence of weaker $\pi\dots\pi$ interaction (distance between $\pi\dots\pi = 3.391\text{\AA}$) and S...S interaction (distance between S...S= 3.461\AA) only in **1c**, which is also a gelator. Therefore, gelation property of **1c** may be attributed to the presence of $\pi\dots\pi$ and S...S interaction.

Table 6.3 Critical analysis of weaker interactions

	1b		1c		1d		3b		3d	
	Bond length (Å ⁰)	Bond angle (°)	Bond length (Å ⁰)	Bond angle (°)	Bond length (Å ⁰)	Bond angle (°)	Bond length (Å ⁰)	Bond angle (°)	Bond length (Å ⁰)	Bond angle (°)
O.....S	2.719		2.675		2.668		2.769		2.696	
Cyclic N- H.....N	2.951	175.93	2.927	150.02	2.955	155.91	2.871	155.91	3.996	148.97
C-H..... π	3.722	158.01								
C-H..... π	3.753	150.02								
C.....O			3.213							
(methyl) C-H.....O			2.683	126.71			3.439	140.25		
$\pi\dots\pi$			3.391							
S...S			3.461							
C-H.....S					3.884	171.84				
C-H.....N					3.428	150.94				
(methyl) C-H..... π									3.685	171.06
(methyl) C-H..... π									3.578	145.49

6.4 Conclusions

A new series of N-(thiazol-2-yl)benzamide derivatives were synthesized and characterized for their gelation behaviour. Out of 12 synthesized compounds only two compounds namely 1c and 3c turned out as gelator, while 2c was unable to demonstrate gelator property. Interestingly steric effect of a methyl group at various positions in thiazole ring and its proximity to electronegative atoms (N or S) in the heterocyclic rings, seems to govern the hydrogen bonding capability of methyl group can be claimed as a main guiding force behind the gelation behaviour of 1c and 3c compounds over 2c. The critical examination of crystal structure of gelator/nongelators were carried out to determine the plausible cause of the gelation behaviour. The investigation of the crystal structures demonstrated presence of weaker $\pi \dots \pi$ and S...S interaction only in **1c**, which is also a gelator. Therefore, gelation property of 1c may be attributed to the presence of $\pi \dots \pi$ and S...S interaction. Furthermore, to study the effect of diamide functionality on gelation behaviour N,N'-di(thiazol-2-yl)phthalamide derivatives were synthesized. None of them could produce gelator assigning that the diamide functionality could not induce the gelation property in present case.

6.5 References

- (1) T. Shiraki, M. Morikawa, N. Kimizuka, *Angew. Chem., Int. Ed.*, **2008**, 47, 106.
- (2) S.J. George, Z. Tomović, M.M.J. Smulders, T.F.A. de Greef, P.E.L.J. Leclère, E.W. Meijer, A.P.H.J. Schenning, *Angew. Chem., Int. Ed.*, **2007**, 46, 8206.
- (3) G.M. Whitesides, J.P. Mathias, C.T. Seto, *Science*, **1991**, 254, 1312.
- (4) K.A. Jolliffe, P. Timmerman, D.N. Reinhoudt, *Angew. Chem., Int. Ed.*, **1999**, 38, 933.
- (5) T. Sugimoto, T. Suzuki, S. Shinkai, K. Sada, *J. Am. Chem. Soc.*, **2007**, 129, 270.
- (6) J.W. Watson, F.C.H. Crick, *Nature*, **1953**, 171, 737.
- (7) D. Seebach, J.L. Matthews, *Chem. Commun.* **1997**, 2015.
- (8) X. Li, Y.-D. Wu, D. Yang, *Acc. Chem. Res.*, **2008**, 41, 1428.
- (9) D.-W. Zhang, X. Zhao, Z.-T. Li, *Acc. Chem. Res.*, **2014**, 47, 7, 1961.
- (10) K. Sakajiri, T. Sugisaki, K. Moriya, *Chem. Commun.*, **2008**, 3447.
- (11) J. Xiao, J. Xu, S. Cui, H. Liu, S. Wang, and Y. Li, *Org. Lett.*, **2008**, 10, 645.
- (12) M. George, R. G. Weiss, *Acc. Chem. Res.*, **2006**, 39, 489.
- (13) M.-O. M. Piepenbrock, G. O. Lloyd, N. Clarke and J. W. Steed, *Chem. Rev.*, **2010**, 110, 1960.
- (14) X. J. Wu, S. J. Ji, Y. Li, B. Z. Li, X. L. Zhu, K. Hanabusa, Y. G. Yang, *J. Am. Chem. Soc.*, **2009**, 131, 5986.
- (15) S. R. Nam, H. Y. Lee and J. I. Hong, *Chem.–Eur. J.*, **2008**, 14, 6040.
- (16) D. R. Trivedi, A. Ballabh, P. Dastidar, *J. Mater. Chem.* **2005**, 15, 2606.
- (17) L. Tao, Z. Huo, S. Dai, J. Zhu, C. Zhang, Y. Huang, B. Zhang, J. Yao, *J. Power Sources*, **2014**, 262, 444.
- (18) N. Díaz, F.-X. Simon, M. Schmutz, M. Rawiso, G. Decher, J. Jestin, P. J. Mézini, *Angew. Chem. Int. Ed.*, **2005**, 44, 3260.
- (19) Q. V. Dolomanov, L. B. Bourhis, R. J. Gildea, J. A. K. Howard, H. Puschmann, *J. Appl. Cryst.*, **2009**, 42, 339.
- (20) G. M. Sheldrick, *Acta Cryst.*, **2008**, A64, 112.
- (21) N. Zweep, A. Hopkinson, A. Meetsma, W. R. Browne, B. L. Feringa, J. H. van Esch, *Langmuir*, **2009**, 25, 8802.